

Depth Estimation in Nighttime using Stereo-Consistent Cyclic Translations

Aashish Sharma¹, Robby T. Tan^{1,2}, and Loong-Fah Cheong¹

¹ECE Department, National University of Singapore, ²Yale-NUS College

aashish.sharma@u.nus.edu, robbly.tan@yale-nus.edu.sg, eleclf@nus.edu.sg

Abstract

Most existing methods of depth from stereo are designed for daytime scenes, where the lighting can be assumed to be sufficiently bright and more or less uniform. Unfortunately, this assumption does not hold for nighttime scenes, causing the existing methods to be erroneous when deployed in nighttime. Nighttime is not only about low light, but also about glow, glare, non-uniform distribution of light, etc. One of the possible solutions is to train a network on nighttime images in a fully supervised manner. However, to obtain proper disparity ground-truths that are dense, independent from glare/glow, and can have sufficiently far depth ranges is extremely intractable. In this paper, to address the problem of depth from stereo in nighttime, we introduce a joint translation and stereo network that is robust to nighttime conditions. Our method uses no direct supervision and does not require ground-truth disparities of the nighttime training images. First, we utilize a translation network that can render realistic nighttime stereo images from given daytime stereo images. Second, we train a stereo network on the rendered nighttime images using the available disparity supervision from the daytime images, and simultaneously also train the translation network to gradually improve the rendered nighttime images. We introduce a stereo-consistency constraint into our translation network to ensure that the translated pairs are stereo-consistent. Our experiments show that our joint translation-stereo network outperforms the state-of-the-art methods.

1. Introduction

Depth from stereo is an important research area in computer vision and is essential for many real-world applications such as autonomous vehicles. Recent developments in deep learning and efforts in creating both synthetic [20, 23] and real-world [21] stereo datasets, have contributed to the advancement of the field. Despite this, depth from stereo under nighttime conditions is still an unexplored area. Conventional non-learning based methods (e.g., [9, 27]) rely on brightness and gradient constancy assumptions, which are

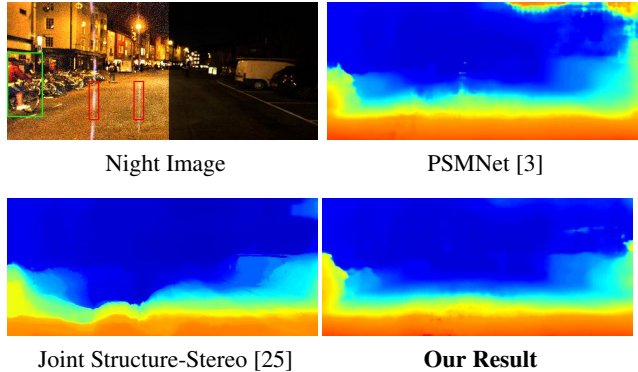


Figure 1. We propose a joint translation-stereo network for nighttime stereo vision. Compared to the existing baseline, Joint Structure-Stereo [25], our result is more accurate and robust to problems such as flares (see the areas marked in red in the night image). It is sharper and has better depth discontinuities (for instance, observe the cyclist marked in green in the night image). Note that, the left half of the night image is boosted with [5] for visualization.

strongly violated due to severe noise, flares, glow, glare, varying illumination, etc. [25]. Fully supervised-learning based methods [3, 15], which are shown to be more effective and efficient in general, suffer from the data-dependency problem. Namely, for optimal results, the networks need to be trained on the same domain of data. If the domain gap between the data used for training and testing is large, then the performance will drop significantly.

As shown in Fig. 1, a state-of-the-art stereo network [3] trained on a daytime dataset, is unable to work properly on nighttime images. This is because nighttime images contain flares, dense noise, glow, glare, etc., which are not present in the daytime training data. One possible solution is to train a network using nighttime images in a fully supervised manner. However, to obtain the disparity ground-truths of nighttime images is not trivial. Maddern et al. [18] create a dataset of 3D point clouds using LIDAR sensors and the corresponding images captured using normal cameras. From this dataset, we can compute the depth of the respec-

tive images. However, these depths are sparse, and cannot capture independently moving objects as well as distant objects. In other words, if we use these depths as ground-truths for training, they will be considerably noisy.

In this paper, our goal is to address the problem of depth from stereo for nighttime images. Our idea is to employ a network that performs image translation from day-to-night (and night-to-day), and stereo matching simultaneously, with the two processes working to benefit each other. We train our translation network to transform original nighttime image pairs to rendered daytime image pairs, and also to transform original daytime image pairs to rendered nighttime image pairs. Simultaneously, we train our stereo network to compute the disparity map of the rendered nighttime image pair, guided by the disparity map computed from the original daytime image pair. Our method uses no direct supervision and thus does not require ground-truths of the nighttime input images.

Unlike the existing translation networks, e.g. CycleGAN [29], our translation network utilizes a stereo-consistency constraint, and translates stereo pairs together instead of individual images. Fig. 2 illustrates the reason of proposing the constraint. From the figure, we can see that since the translation network CycleGAN translates images individually, it generates the stereo pair inconsistently i.e. the image structures are inconsistent across the stereo pair (Fig. 2b), which negatively affects the disparity computation (Fig. 2d). In contrast, our translation network, which is trained with the stereo-consistency constraint and translates the stereo pair together, can reduce these inconsistencies (Fig. 2c) and generates a more robust result (Fig. 2e). Fig. 1 shows that our method outperforms the state-of-the-art methods in general stereo vision [3] and in nighttime stereo vision [25].

To summarize, our main contributions are as follows:

- We introduce an end-to-end learning-based method to address the problem of nighttime stereo vision. Additionally, our method uses no direct supervision and does not need ground-truth disparities for training on nighttime images.
- We propose a novel idea of using a joint network that performs translation and stereo matching simultaneously. Our experiments confirm that compared to the individual approaches, our joint network generates stereo-consistent translations and provides better disparity results.
- We introduce a stereo-consistency constraint into the translation network to ensure that it generates translations stereo-consistently, namely, the stereo images in each rendered pair contain consistent image contents/structures, which is imperative for stereo matching.
- We address the limitations of the current state-of-the-art

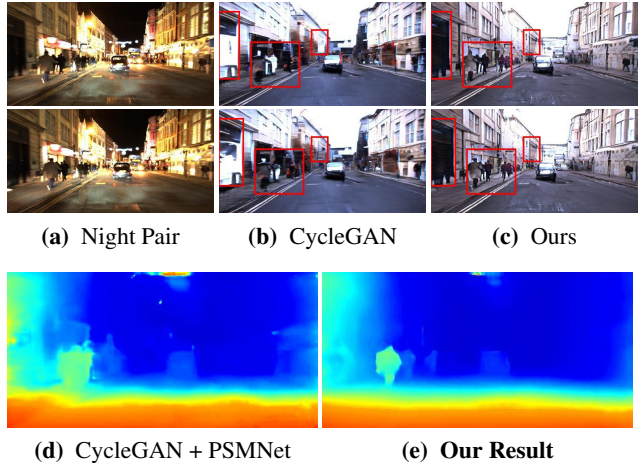


Figure 2. Example showing the benefits of using the stereo-consistency constraint into the translation network. For the given night pair, compared to CycleGAN [29], our translations have lesser inconsistencies (compare the marked areas between (b) and (c)), leading to a more robust disparity result. Note that, we use the same stereo network, PSMNet [3], to generate the disparity results.

methods on nighttime stereo vision. Our method significantly outperforms them in both the computational efficiency and the estimated disparity accuracy, particularly for robustness to glow, streak-like flares and high-glare.

2. Related Work

Depth from stereo has been investigated extensively, and for comprehensive review we refer to Scharstein et al.’s [24] and Hirschmuller et al.’s [10]. Some recent learning based methods (e.g., [15, 3]) have achieved state-of-the-art performance on the KITTI daytime stereo dataset [21]. Nighttime stereo vision however, is a relatively less investigated topic given its numerous challenges. Hence, despite its significance, there are only few methods that have attempted to address the problem [8, 12, 25]. Both Heo et al. [8] and Jiao et al. [12] assume the noise distribution to be Gaussian, and thus do not generalize well on nighttime images. Moreover, Heo et al.’s [8] is limited to only low Gaussian noise levels (st.d. ≤ 25).

Sharma and Cheong’s [25] attempts to address this problem by optimizing a joint structure-stereo model that performs structure extraction and stereo estimation jointly. There is no explicit assumption on the noise distribution, and hence, the method generalizes well on nighttime images, and it is the current state-of-the-art method. However, owing to its high optimization complexity, it is computationally inefficient, and still suffers from other nighttime problems such as flares, glare, etc.

Our proposed model has similar key insights to Hoffman

et al.’s [1] and Sharma and Cheong’s [25]. Like the structure extraction part of [25], we enforce the stereo-consistency constraint during the translation process by including the constraint into the translation network. Our translation step is similar to that used in [1] but with two key differences: 1) Our translation network includes the stereo-consistency constraint and translates stereo pairs together, while [1] models semantic-consistency on individual images. 2) Unlike [1], we do not use the same pre-trained task network (stereo for ours, semantic segmentation for [1]) for the two domains (source and target) to enforce our mentioned constraint.

We consider that given the complications in the nighttime conditions, the domain gap between our day (source) and night (target) images can be larger than the domain gap in [1], and thus a single task network might not suffice. For this reason, we use two identical task networks for our two domains respectively. As in [1], one is pre-trained on the source data, but the other is trained jointly with the translation network on the translated data using the disparity supervision from the corresponding source data.

3. Our Method

Our problem statement is as follows. We have two input domains - day and night. Both input domains have sets of stereo image pairs available, represented by (X_D^L, X_D^R) and (X_N^L, X_N^R) , where the subscript defines the domains ($D = \text{daytime}$, and $N = \text{nighttime}$) and the superscript defines the left/right image view. All stereo image pairs in the sets are rectified. A stereo pair drawn from the sets is represented by small letters: (x_D^L, x_D^R) for a daytime pair and (x_N^L, x_N^R) for a nighttime pair.

The two input domains are uncorrelated. For any stereo pair in the daytime domain, we do not have its exact corresponding pair in the nighttime domain (and vice-versa). Moreover, we assume that we have the disparity ground-truths available for the daytime domain, represented by Y_D^L . However, we do not have the ground-truths for the nighttime domain. Our goal is to estimate the disparity map of a given nighttime pair, (x_N^L, x_N^R) .

To achieve the goal, we propose a joint network consisting of two subnetworks: translation and stereo networks. Our translation network is represented by $\{(g_D, d_D), (g_N, d_N)\}$ with g and d being the generator and discriminator networks respectively. Our stereo part contains two identical networks, $\{f_D, f_N\}$, each modelled on PSMNet [3], which has recently achieved state-of-the-art results on the KITTI [21] daytime stereo dataset.

Fig. 3 shows our network architecture. It has two concurrent training cycles: The one at the top row performs the day \rightarrow night translation, and the one at the bottom row performs the night \rightarrow day translation. While we draw two separate cycles in the figure, the top and bottom networks

are one (same) network. In our method, we assume that we have already pre-trained f_D on the daytime stereo training data, and also initialized f_N with f_D ’s trained weights. Since we do not need f_D to learn any further for the daytime domain, we keep it completely frozen in the two cycles. For f_N , in the first cycle (the top row of Fig. 3), we train it together with g_D on the translated nighttime image pairs using the disparity supervision from their input daytime counterparts. However, we freeze f_N in the second cycle (the bottom row of Fig. 3), since we have no disparity ground-truths available for the input nighttime image pairs. The details of the steps are discussed as follows:

3.1. Pre-Training Stage

We train f_D on the daytime input image pairs, (X_D^L, X_D^R) , using their corresponding disparity ground-truths, Y_D^L . We use the multi-branch loss function from [3], i.e. for (x_D^L, x_D^R) drawn from (X_D^L, X_D^R) and y_D^L drawn from Y_D^L , the loss is expressed as:

$$\mathcal{L}_{\text{stereo}}(f_D) = \mathbb{E}_{(x_D^L, x_D^R), y_D^L} \left[\sum_{k=1}^3 w_k \cdot \|y_{kD}^L - y_D^L\|_1 \right], \quad (1)$$

where $f_D[(x_D^L, x_D^R)] = \{y_{kD}^L\}_{k=1,2,3}$ represent the three prediction branches from the stacked hourglass model of f_D . w_k is the scaling weight of the associated loss term. Having trained f_D , we freeze its weights completely.

3.2. Training Stage

The stereo network f_N is initialized with the pre-trained weights of f_D , and the translation network, $\{(g_D, d_D), (g_N, d_N)\}$, is randomly initialized.

First Training Cycle In the first training cycle (day \rightarrow night), given any daytime image pair (x_D^L, x_D^R) and any nighttime image pair (x_N^L, x_N^R) , the rendered nighttime pair is generated by the daytime generator: $(\hat{x}_N^L, \hat{x}_N^R) = g_D[(x_D^L, x_D^R)]$, where (g_D, d_D) are trained using the following loss functions:

$$\mathcal{L}_{\text{GAN}}(g_D) = \mathbb{E}_{(x_D^L, x_D^R)(x_N^L, x_N^R)} [(d_D[(\hat{x}_N^L, \hat{x}_N^R)] - d_D[(x_N^L, x_N^R)] - 1)^2], \quad (2)$$

$$\mathcal{L}_{\text{GAN}}(d_D) = \mathbb{E}_{(x_D^L, x_D^R)(x_N^L, x_N^R)} [(d_D[(x_N^L, x_N^R)] - d_D[(\hat{x}_N^L, \hat{x}_N^R)] - 1)^2], \quad (3)$$

where we use the least-squares adversarial loss [19], which is adapted to the recently proposed relativistic loss formulation [14] to stabilize the training process.

We further translate the rendered nighttime image pair $(\hat{x}_N^L, \hat{x}_N^R)$ to the rendered daytime image pair $(\tilde{x}_D^L, \tilde{x}_D^R)$ using the nighttime generator: $(\tilde{x}_D^L, \tilde{x}_D^R) = g_N[(\hat{x}_N^L, \hat{x}_N^R)]$. Based on the cycle-consistency constraint [29], we expect that the rendered daytime image pair $(\tilde{x}_D^L, \tilde{x}_D^R)$ should be

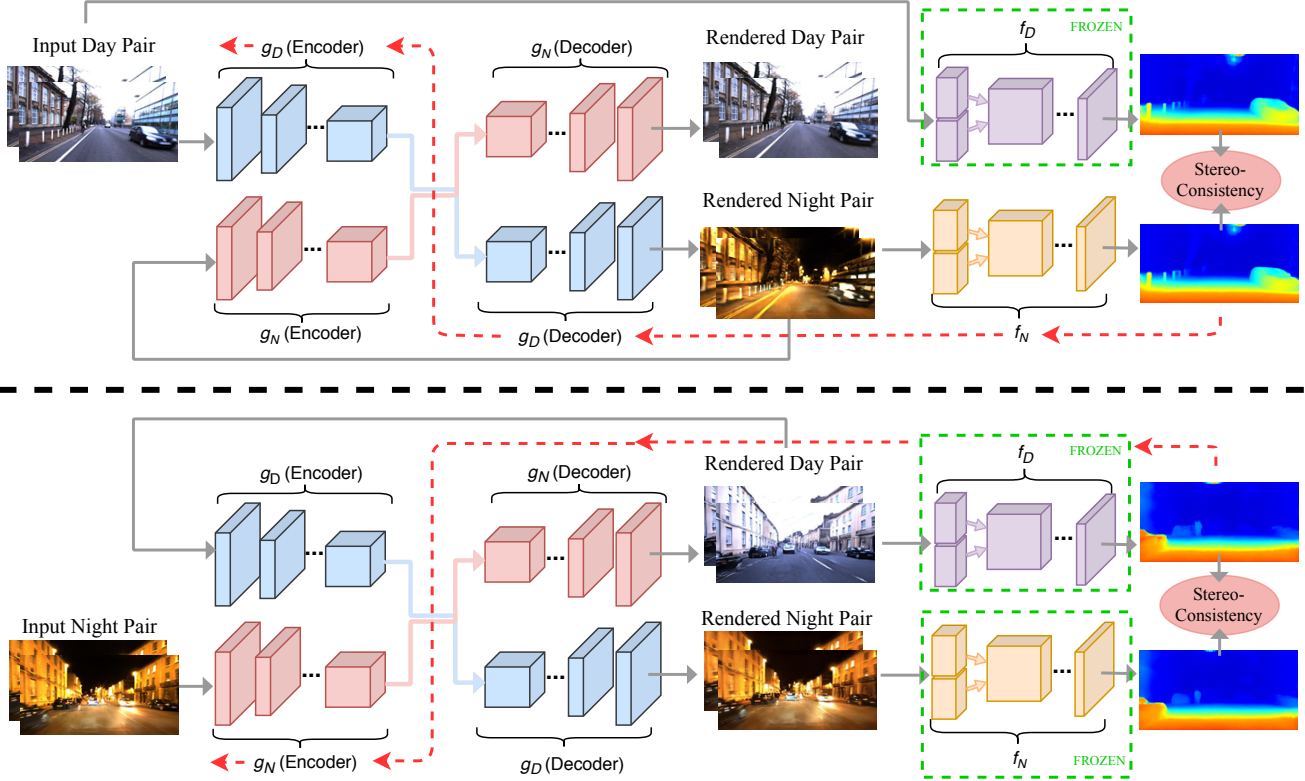


Figure 3. The two concurrent training cycles of our joint network are shown in the top and bottom rows respectively. For the sake of illustration of the stereo-consistency loss, discriminators and the other losses are omitted. In the first cycle, where we have day→night translation, enforcing the stereo-consistency constraint, we jointly train g_D and f_N . This ensures that g_D generates stereo-consistent translations, while f_N is getting trained on them. In the second cycle, where we have night→day translation, we train g_N with the stereo-consistency constraint. To elucidate the usage of the stereo-consistency constraint, we have red-dotted arrows showing the associated back-propagation directions and green-dotted rectangles marking the frozen stereo networks used in the two cycles.

the same as the original daytime image pair (x_D^L, x_D^R) . Thus we can define a cycle-consistency loss function to train the daytime generator, g_D :

$$\mathcal{L}_{\text{cyc-con}}(g_D) = \mathbb{E}_{(x_D^L, x_D^R)} [\|\tilde{x}_D^L - x_D^L\|_1 + \|\tilde{x}_D^R - x_D^R\|_1]. \quad (4)$$

Now, we introduce the stereo-consistency constraint. The idea is that the disparity computed from the rendered nighttime image pair $(\hat{x}_N^L, \hat{x}_N^R)$ should be the same as the disparity computed from the original daytime image pair (x_D^L, x_D^R) , since they are originated from the same images. As a result, we can train f_N based on this stereo-consistency constraint (see the top row of Fig. 3). Specifically, using $f_D[(x_D^L, x_D^R)] = \{y_k^L\}_{k=1,2,3}$ as supervision, and $f_N[(\hat{x}_N^L, \hat{x}_N^R)] = \{\hat{y}_k^L\}_{k=1,2,3}$ as prediction, we have the following stereo-consistency loss function to train (g_D, f_N) :

$$\mathcal{L}_{\text{ste-con}}(g_D, f_N) = \mathbb{E}_{(\hat{x}_N^L, \hat{x}_N^R), y_k^L} \left[\sum_{k=1}^3 \|\hat{y}_k^L - y_k^L\|_1 \right]. \quad (5)$$

This completes the training procedure of the first cycle. As we can see, the stereo-consistency constraint in the first cycle acts as the coupling link between the two processes in our joint network.

Second Training Cycle In this cycle, we perform night→day translation. The process is similar to the first training cycle, and so the loss functions. $\mathcal{L}_{\text{GAN}}(g_N)$, $\mathcal{L}_{\text{GAN}}(d_N)$, $\mathcal{L}_{\text{cyc-con}}(g_N)$ for (g_N, d_N) , are obtained from Eqs. (2), (3), and (4) by simply swapping the domain labels from daytime to nighttime.

The stereo-consistency loss in this cycle is also similar to Eq. (5), where we expect the disparity computed from the rendered daytime image pair, $(\hat{x}_D^L, \hat{x}_D^R)$, to be the same as the disparity computed from the original nighttime image pair, (x_N^L, x_N^R) . However, there are two important changes. First, we do not train f_N this time as there is no disparity ground-truth available for the input nighttime image pair (x_N^L, x_N^R) . Second, for the stereo-consistency loss, we compute the disparity from the rendered nighttime image

pair $(\tilde{x}_N^L, \tilde{x}_N^R)$, instead of the original nighttime image pair (x_N^L, x_N^R) (see the bottom row of Fig. 3).

The reason is because in the beginning of the training process, the rendered nighttime image pair in the first cycle $(\hat{x}_N^L, \hat{x}_N^R)$ is different from the original nighttime image pair (x_N^L, x_N^R) , yet it is more similar to the rendered nighttime image pair in the second cycle, $(\tilde{x}_N^L, \tilde{x}_N^R)$. Since, both of them are synthetically rendered image pairs.

Moreover, the two synthetically rendered pairs $\{(\hat{x}_N^L, \hat{x}_N^R), (\tilde{x}_N^L, \tilde{x}_N^R)\}$ are likely to be more stereo-consistent than the rendered nighttime image pair and original nighttime image pair $\{(\hat{x}_N^L, \hat{x}_N^R), (x_N^L, x_N^R)\}$, because of random noise present in the original images. Using the rendered night pairs, we can get a more stable learning process (as shown in our ablation study). Therefore, using $f_N[(\tilde{x}_N^L, \tilde{x}_N^R)] = \{\tilde{y}_{kN}^L\}_{k=1,2,3}$ as supervision, and $f_D[(\hat{x}_D^L, \hat{x}_D^R)] = \{\hat{y}_{kD}^L\}_{k=1,2,3}$ as prediction, we have the following stereo-consistency loss function to train g_N :

$$\mathcal{L}_{\text{ste-con}}(g_N) = \mathbb{E}_{(\hat{x}_D^L, \hat{x}_D^R), \tilde{y}_{kN}^L} \left[\sum_{k=1}^3 \|\hat{y}_{kD}^L - \tilde{y}_{kN}^L\|_1 \right]. \quad (6)$$

This completes the training procedure of the second cycle.

Putting together all our loss functions, we can express it as:

$$\begin{aligned} \mathcal{L}_{\text{All}}(g_D, g_N, d_D, d_N, f_N) &= \mathcal{L}_{\text{GAN}}(g_D) + \mathcal{L}_{\text{GAN}}(g_N) \\ &+ \lambda_{\text{cyc}} \mathcal{L}_{\text{cyc-con}}(g_D) + \lambda_{\text{cyc}} \mathcal{L}_{\text{cyc-con}}(g_N) + \lambda_{\text{ste}} \mathcal{L}_{\text{ste-con}}(g_N) \\ &+ \lambda_{\text{ste}} \mathcal{L}_{\text{ste-con}}(g_D, f_N) + \mathcal{L}_{\text{GAN}}(d_D) + \mathcal{L}_{\text{GAN}}(d_N), \end{aligned} \quad (7)$$

where λ_{cyc} and λ_{ste} are the scaling weights of the two consistency loss functions respectively. Minimizing Eq. (7) gives us the optimized networks g_D^*, g_N^* and f_N^* . As a result, we can get the final disparity result on a given nighttime image pair, (x_N^L, x_N^R) , by applying $f_N^*[g_D^*[g_N^*[(x_N^L, x_N^R)]]]$, which produces the estimated disparity map $\{y_{3N}^L\}$. The whole process is summarized in Algorithm 1.

4. Implementation

4.1. Network Architecture

Our translation network consists of two generators and two discriminators (one for each domain), and each generator further comprises of an encoder-decoder as shown in Fig. 3. The encoder consists of three convolution layers and four residual blocks [7], while the decoder consists of four residual blocks followed by two deconvolution and one convolution layers. Each discriminator comprises of three independent sub-discriminators comparing three components of the input images respectively - ‘Blurred-RGB’ (RGB images blurred with a 5×5 Gaussian kernel), ‘Grayscale’ (luminance channel), and ‘Gradients’ (horizontal and vertical gradients) [2]. Each sub-discriminator is a 32×32 PatchGAN [11], containing five convolution layers.

Algorithm 1 Depth Estimation in Nighttime using Stereo-Consistent Cyclic Translations

- 1: Given daytime pairs (X_D^L, X_D^R) with disparity labels Y_D^L , and nighttime pairs (X_N^L, X_N^R) with no labels.
 - 2: **Pre-Training Stage:**
 - 3: Initialize f_D with random weights.
 - 4: With $(x_D^L, x_D^R) \sim (X_D^L, X_D^R)$ and $y_D^L \sim Y_D^L$, train f_D by minimizing Eq. (1). Freeze the weights of the optimized network f_D^* .
 - 5: **Training Stage:**
 - 6: Initialize f_N with the weights of f_D^* , and $\{(g_D, d_D), (g_N, d_N)\}$ with random weights.
 - 7: With $(x_D^L, x_D^R) \sim (X_D^L, X_D^R)$ and $(x_N^L, x_N^R) \sim (X_N^L, X_N^R)$, train $\{(g_D, d_D), (g_N, d_N)\}$ and f_N jointly by minimizing Eq. (7). Obtain the optimized networks g_D^*, g_N^* and f_N^* .
 - 8: **Testing Stage:** Given a nighttime pair (x_N^L, x_N^R) , obtain its disparity result $\{y_{3N}^L\}$ by $\{y_{3N}^L\} = f_N^*[g_D^*[g_N^*[(x_N^L, x_N^R)]]]$.
-

Our two stereo networks are based on the stacked hourglass architecture of PSMNet [3]. Each stereo network has three convolution layers with four residual blocks, followed by a Spatial Pyramid Pooling [6] module for feature extraction. The features extracted from a stereo pair are concatenated into a 4D cost volume, which is regularized by a 3D convolution architecture consisting of repeated top-down (stacked hourglass) processing. The last layer is disparity regression [15], to generate the final disparity prediction.

4.2. Training Parameters

For all the experiments we use images resized to 256×512 (due to our limited memory size), and hyper-parameters $\{w_1, w_2, w_3, \lambda_{\text{cyc}}, \lambda_{\text{ste}}\} = \{0.5, 0.7, 1, 10, 0.05\}$. To accommodate the stereo pair requirement, our translation network is simply modified to have two exactly similar weight-sharing pipelines, each working on an image from the pair. We use a buffer of 50 previously translated pairs to reduce model oscillations [4, 26]. All networks use Adam [16] solver with its parameters $\{\beta_1, \beta_2\} = \{0.5, 0.999\}$. We use a batch size of 4, and keep a constant learning rate of 0.0002 for all the networks for the first-half of the training epochs, and then linearly decay it to zero over the second-half.

5. Experiments

In this section, we evaluate the performance of our method through a series of experiments. Our quantitative evaluation is based on the percentage of bad-pixels [21], governed by the error threshold δ (in pixels).

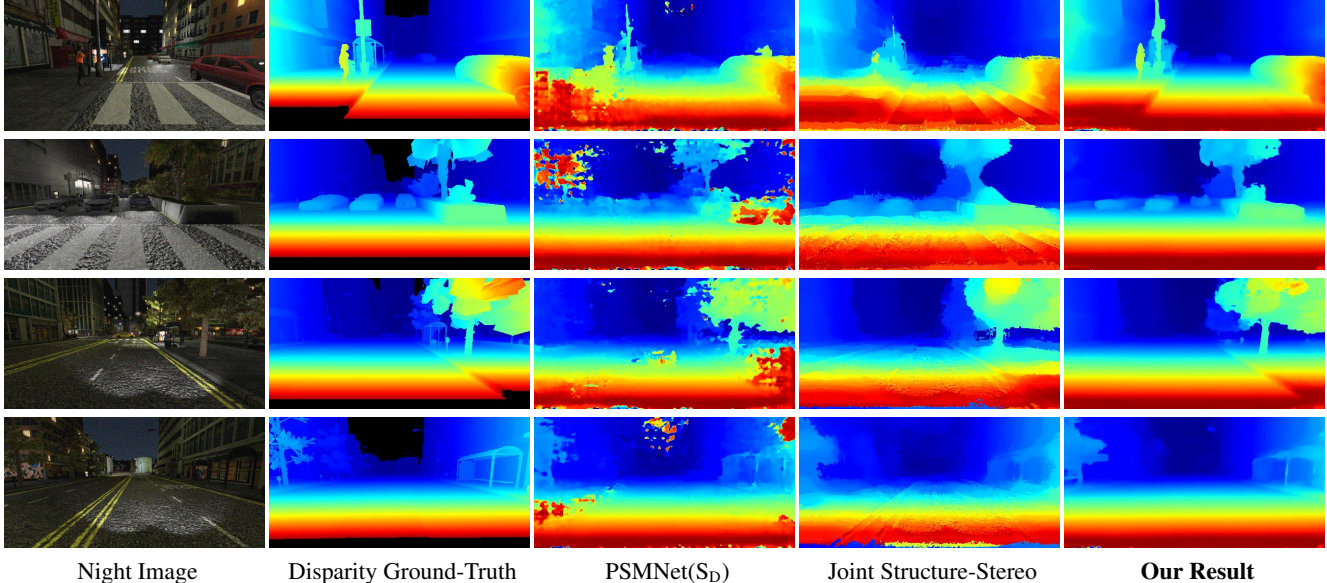


Figure 4. Qualitative results on the SYNTHIA night test data. Our results are sharper and more accurate than the baseline methods.

Table 1. Quantitative results on the SYNTHIA night test data.

	$\delta=1$	$\delta=2$	$\delta=3$
PSMNet(S_D)	36.16	26.83	21.48
CycleGAN + PSMNet(S_D)	30.28	22.65	18.25
Joint Structure-Stereo[25]	29.42	22.16	16.39
Ours	14.23	8.92	6.48
PSMNet(S_N)	5.24	2.97	2.13

5.1. Results on Synthetic Night Data

For our first experiment, we use the SYNTHIA [23] dataset, which provides daytime and nighttime synthetic stereo data, and accurate dense disparity ground-truths. However, it does not realistically represent the complex attributes of real nighttime images such as noise, flares, glow and glare.

We take 3800 stereo pairs (3500 for training and validation; 300 for testing) from the two data each, and add a small amount of random Gaussian noise (st.d. $\in [10, 25]$) in the nighttime image pairs to roughly simulate the low SNR conditions present in real nighttime images. The training process follows the methodology presented in Sec. 3. The main training stage runs for 40 epochs and takes ~ 25 hours on four nVidia GTX 1080Ti GPUs to complete.

For comparisons, we select the following baselines: 1) ‘PSMNet(S_D)’, PSMNet [3] trained on the SYNTHIA daytime data. 2) ‘CycleGAN + PSMNet(S_D)’, CycleGAN [29]

to translate the SYNTHIA nighttime images into daytime images, which are then used on ‘PSMNet(S_D)’. 3) Joint Structure-Stereo [25], a state-of-the-art method for nighttime stereo vision. And, 4) ‘PSMNet(S_N)’, PSMNet [3] trained on the SYNTHIA nighttime data, which acts as the “oracle” method. We show the results of ‘PSMNet(S_N)’ to observe how our method performs with respect to the “ideal” case. Qualitative results are shown in Fig. 4 (see Fig. 9 for comparison with the individual approach ‘CycleGAN + PSMNet(S_D)’). Quantitative results are presented in Table. 1. From the results, we can observe that our method generates disparity predictions which are sharper and more accurate than the baseline methods.

5.2. Results on Real Night Data

We test our model on real night data. For this, we select the Oxford RobotCar [18] dataset. It provides a large amount of stereo data captured in daytime and diverse nighttime conditions, and also provides their raw sparse (LIDAR-based) disparity ground-truth maps. However, given the various limitations of LIDAR (erroneous for transparent, independently moving objects), this ground-truth is not suitable for training, until manually processed (as done in [21]). Therefore, in the pre-training stage, for training f_D , we start with the KITTI [21] daytime dataset that provides 200 stereo pairs with their processed disparity ground-truth maps. We then generalize it on the Oxford daytime dataset using the zoom-and-learn trick proposed in [22]. This simple trick leads to finer and more accurate predictions on the Oxford daytime data. The main training

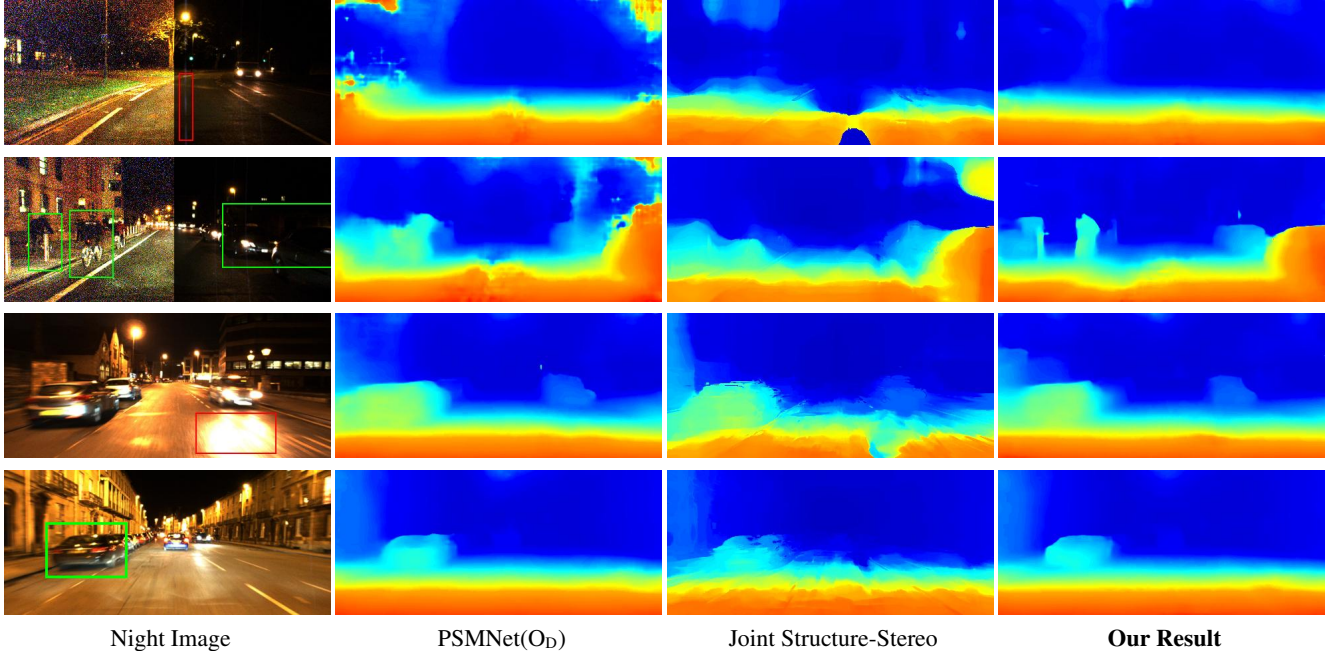


Figure 5. Qualitative results on the Oxford night test data. Our results are robust to problems such as flares and high glare (see the areas marked in red in the night images). Additionally, they are sharper and have better depth discontinuities (for instance, observe the cyclists, pedestrians and other regions marked in green in the night images).

Table 2. Quantitative results on the Oxford night test data.

	Oxford (P-L)		Oxford (W-L)	
	$\delta=3$	$\delta=5$	$\delta=3$	$\delta=5$
PSMNet(O _D)	16.58	7.17	8.24	3.82
CycleGAN + PSMNet(O _D)	39.96	20.33	20.97	8.59
PSMNet(S _N)	35.17	22.19	9.36	5.60
Joint Structure-Stereo[25]	12.75	5.09	7.92	2.88
Ours	9.65	3.83	7.71	3.67

stage then follows the process mentioned in Sec. 3. For this, we take 9000 daytime and 8600 nighttime pairs for training, and additional 1000 nighttime pairs for validation¹. We also ensure that the night pairs cover a variety of nighttime conditions such as poorly-lit to well-lit, flares, low-to-high glow and glare. The main training stage runs for 40 epochs and takes ~ 60 hours. We then test our optimized model on 250 additional nighttime pairs, 125 from poorly-lit scenes (referred as Oxford(P-L)), and the other 125 from well-lit scenes (referred as Oxford(W-L)).

For comparison, we have the following baselines: 1) ‘PSMNet(O_D)’, PSMNet [3] generalized on the Oxford

¹Our evaluation on the Oxford dataset, whether during validation or testing, is based on the assumption that the raw ground-truth is mostly correct, i.e. it is accurate for most of the points in the scene (especially for static objects such as buildings, roads, etc.)

daytime data (as discussed above). 2) ‘CycleGAN + PSMNet(O_D)’, CycleGAN [29] to translate the Oxford nighttime images into daytime images, which are then used on ‘PSMNet(O_D)’. 3) ‘PSMNet(S_N)’. And, 4) Joint Structure-Stereo [25], a state-of-the-art method for nighttime stereo vision. Quantitative results are shown in Table. 2. Qualitative comparisons are shown in Fig. 5.

We can observe that compared to ours, ‘PSMNet(S_N)’ performs poorly on real nighttime images. This is due to the domain gap problem that arises on training on synthetic data and testing using real data. A similar domain gap problem exists for ‘PSMNet(O_D)’. Since it is trained on daytime images, it cannot handle problems such as noise, flares, etc. present in real nighttime images, and produces blurry and incorrect results. We again obtain a better performance than the competing individual approach, ‘CycleGAN + PSMNet(O_D)’, which highlights the benefits of our joint network using our stereo-consistency constraint (see Fig. 2 and Fig. 9 for comparisons between our joint network and the individual approach). Our results are stable under a variety of nighttime conditions such as poorly-lit (top two rows, Fig. 5, left-half of the night images boosted for visualization) to well-lit scenes (bottom two rows, Fig. 5). Our results are more accurate and have sharper boundaries than the baseline methods (see the marked areas in green in the night images, Fig. 5). They are robust to flares and high glare (see the marked areas in red in the night images,

Algorithm 2 Data Augmentation: Creating Synthetic Glow Patterns in Daytime Images

- 1: Given daytime pairs (X_D^L, X_D^R) with disparity labels Y_D^L . Let $(x_D^L, x_D^R) \sim (X_D^L, X_D^R)$ and $y_D^L \sim Y_D^L$.
 - 2: **Initialization:**
For $n \geq 0$ glow patterns to be synthesized, define their positions \mathbf{p} and sizes \mathbf{s} .
 - 3: **for** $i = 1 : n$ **do**
 - 4: **For** $\mathbf{p}_i \in \mathbf{p}$ and $\mathbf{s}_i \in \mathbf{s}$, let $r_{o_i} \sim \text{randi}(\mathbf{s}_i - 5, \mathbf{s}_i)$, $r_{m_i} \sim \text{randi}(r_{o_i} - 5, r_{o_i})$, and $r_{i_i} \sim \text{randi}(r_{m_i} - 15, r_{m_i} - 10)$.
 - 5: Let o_i , m_i and i_i be circular patterns of colors red, yellow and white, and radii r_{o_i} , r_{m_i} and r_{i_i} respectively. The patterns are blurred with Gaussian kernels of size r_{o_i} , 10 and 5 respectively.
 - 6: Generate the glow pattern g_i at position \mathbf{p}_i by $g_i = o_i + m_i + i_i$.
 - 7: Modify x_D^L by $x_D^L = (1 - m_{g_i}) \odot x_D^L + m_{g_i} \odot g_i$, where \odot represents the element-wise product, and $m_{g_i} \in [0, 1]$ is a mask to blend g_i and x_D^L together.
 - 8: Using y_D^L , warp g_i and m_{g_i} towards x_D^R . Using the warped g_i and m_{g_i} , modify x_D^R similarly as x_D^L .
 - 9: **end for**
-

Fig. 5). Additionally, our model is efficient and it only takes <0.4 secs (tested on GPU) to generate a result, while the existing state-of-the-art [25] takes about ~ 3 -4mins (tested on CPU). To facilitate future research, our code will be publicly available.

6. Discussion

Our experiments show that our method outperforms the state-of-the-art method [25] and other baseline methods qualitatively and quantitatively on the synthetic and real night data. However, like current deep learning methods, our method depends on the training data. Specifically, if the two domains of the training data for the translation network have similar objects (e.g., cars, buildings, roads, pedestrians, cyclists, etc.), then our disparity estimation can be robust, since the translated or rendered object structures are the same as the original ones.

However, if an object in one domain is often wrongly mapped to a different object in the other domain, then the translation network can be trapped into associating the two different objects as the same object. To the best of our knowledge, this is a known open problem in unpaired image translation [29, 17, 28]. In our case of nighttime-daytime translation, glow in nighttime images does not have the corresponding phenomenon in daytime; what’s worse, it is wrongly mapped to trees most of the time. Consequently, our network generates wrong depth estimation, since it learns wrongly about the depth of glow. Recall that



(a) Original Day Image (b) Augmented Day Image

Figure 6. An example showing glow rendering in daytime images using our data augmentation method. (a) Original daytime image from the Oxford dataset [18]. (b) Augmented daytime image with rendered glow patterns.

in our framework in Fig. 3, the supervision of our stereo-consistency loss is from daytime images that do not have glow, and often have trees in the associated glow regions. The top row of Fig. 7 shows an example where glow is wrongly translated to a tree (Fig. 7b). As a result, the depth in the glow region is wrongly estimated (Fig. 7c).

To handle the false translation problem associated with glow, we propose a simple yet effective strategy based on data augmentation. Specifically, we augment the daytime images by creating synthetic glow patterns in them². This reduces the domain gap between the daytime and nighttime images. It also ensures that the rendered nighttime images contain glow patterns of different sizes and on different background objects, since the synthetic glow patterns we create in the daytime images are randomly sized and positioned. This is needed because glow is a freely occurring phenomenon, which means that it can be present anywhere in a scene, be in front of buildings, trees, sky, etc. When glow is associated with different background objects (and not just trees), our stereo network can learn to recover the true depth of glow, which is the depth of the background object containing the glow. The entire data augmentation procedure is described in Algorithm 2. An example of data augmentation is shown in Fig. 6.

We test our method on the augmented Oxford dataset. The bottom row of Fig. 7 shows the new results. We can see that now our translation network does not map the glow region into a tree in the rendered daytime image (Fig. 7e), and instead maps it into a synthetic glow pattern. This shows that we can reduce the problem of fake translation by ensuring that the two domains contain similar objects/structures. The new disparity result (Fig. 7f) for the glow region is also better and more reliable than the previous result. The new depth result resembles more like the depth of the background object, which is a wall in this example. Some sample rendered images for the augmented Oxford dataset are also shown in Fig. 8 for reference.

We also investigated why the false translation problem

²Note that, we do not need a very accurate model for creating synthetic glow in the daytime images, since our translation network can learn to map it into realistic glow in the rendered nighttime images, as shown in Fig. 8.



Figure 7. Top row: We show the possibility of getting false depth estimates for glow regions. As shown, this can happen when the glow region gets wrongly translated into a different object such as a tree. Bottom row: We handle the problem with data augmentation, i.e. by creating synthetic glow patterns in the daytime images. Our translation network now maps the glow region into a synthetic glow pattern, and the new disparity result is improved and closer to the sparse ground-truth. Note that, the disparity patches are scaled for visualization.

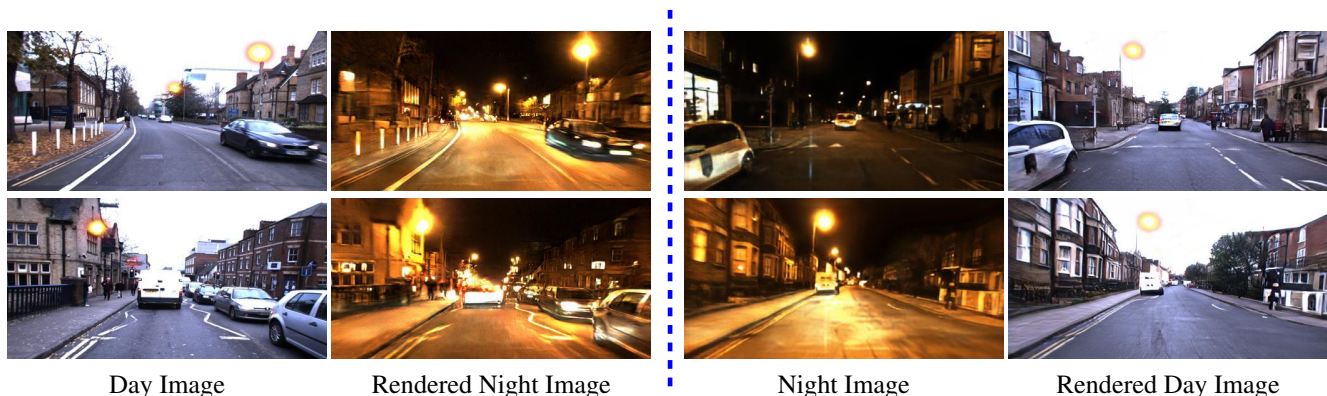


Figure 8. Examples of rendered images obtained from our translation network for the Oxford dataset. Note that, the daytime images are augmented to have synthetic glow patterns.

is not prominent for other nighttime phenomenon such as glare and flare. We find that unlike glow, glare in the Oxford dataset usually occurs on either roads or buildings (as can be seen in Fig. 5 and Fig. 8). This strong association allows the translation network to map the glare regions to the underlying objects. Even though the mapping might contain wrong disparity information (as glare might violate constancy constraints), we understand that our stereo network can draw upon the disparity information of the surrounding region in the underlying object, to correct disparity in the mapped glare region. In contrast, glow moves freely across the background objects, be they sky, trees, or buildings. Thus the mapped fake object (tree) is also freely floating, rather than being associated with some larger substrates whose disparities can be leveraged to produce correct disparities for the glow region.

Flare as a nighttime phenomenon would seem to be closer to glow than glare (in the sense that it is also not attached to a substrate). However, in the Oxford dataset, flares usually are in the form of thin streaks that run vertically across sky and roads (as can be seen in Fig. 5). Perhaps due to their thin shape, and their association with these background objects and the mapping being embedded within these larger regions, the disparities produced can correctly follow that of the sky or road, as the case may be.

7. Ablation Study

Learning stabilization We show that the learning process is stabilized when the rendered nighttime pair $(\tilde{x}_N^L, \tilde{x}_N^R)$ is used instead of the real nighttime pair (x_N^L, x_N^R) for the stereo-consistency constraint in the second training cycle. From Fig. 10a, we can observe that when the ren-

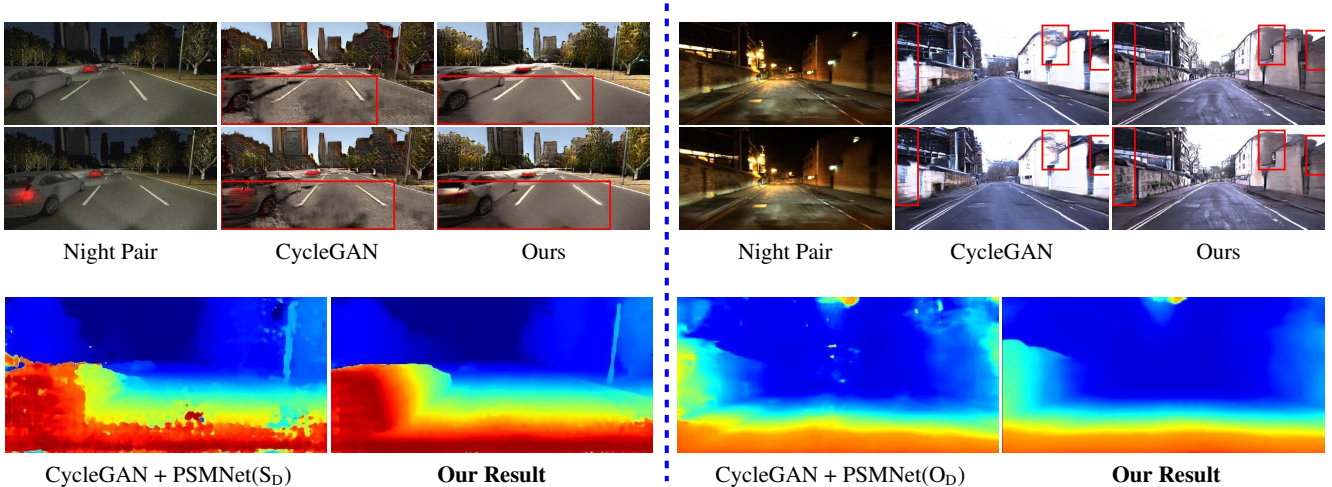


Figure 9. Qualitative comparison of our method with the individual approaches ‘CycleGAN + PSMNet(S_D)’ and ‘CycleGAN + PSMNet(O_D)’ on the SYNTHTIA (left side) and Oxford (right side) datasets respectively. Compared to the individual approaches, our method using our stereo-consistency constraint generates translations with lesser inconsistencies (compare the marked areas between the rendered pairs generated by CycleGAN and our method). This makes our method to produce better disparity results than the individual approaches.

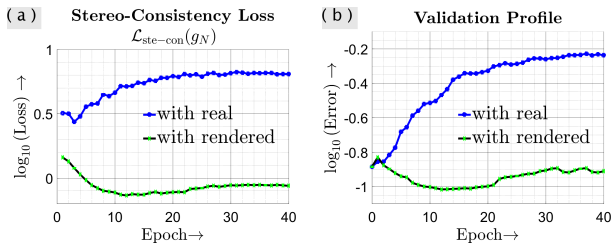


Figure 10. Learning stabilizes and the stereo-consistency loss $\mathcal{L}_{ste-con}(g_N)$ reduces gradually when the rendered nighttime pair is used instead of the real nighttime pair (see (a)). The corresponding validation profiles are also shown in (b). The plots are from our experiment on the Oxford dataset.

dered nighttime pair is used, the stereo-consistency loss $\mathcal{L}_{ste-con}(g_N)$ reduces gradually as expected. However, it diverges when the real nighttime pair is used. This, as mentioned, is because in the beginning of the training process, the rendered nighttime pair in the first cycle (\hat{x}_N^L, \hat{x}_N^R) is more similar to the rendered nighttime pair in the second cycle ($\tilde{x}_N^L, \tilde{x}_N^R$) than the real nighttime pair (x_N^L, x_N^R). Using this similarity stabilizes the learning process, The validation profiles shown in Fig. 10b also confirm the same.

Varying the strength of stereo-consistency We check the variation of the best test performance (for $\delta=3$) on the Oxford dataset with λ_{ste} , the parameter controlling the strength of our stereo-consistency constraint. We observe that it is $\{12.46, 11.18, \mathbf{8.81}, 10.92, 12.46\}$ for $\lambda_{ste} =$

$\{0, 0.01, \mathbf{0.05}, 1, 10\}$, thus making $\lambda_{ste}=0.05$ as our default and optimal setting of this parameter.

8. Conclusion

In this paper, we have proposed a novel joint translation and stereo network to address the problem of depth from stereo in nighttime. For this, we have introduced a stereo-consistency constraint into the translation network so as to generate meaningful stereo-consistent translations, which as we have shown, is imperative for stereo matching. We have showed through experiments our method’s capability to work robustly in varying nighttime conditions, ranging from poorly-lit to well-lit scenes. It can handle various limitations of the present baseline methods in terms of both efficiency and stereo quality, particularly for robustness to glow, streak-like flares and high glare.

References

- [1] Cycada: Cycle consistent adversarial domain adaptation. In *International Conference on Machine Learning (ICML)*, 2018.
- [2] A. Anoosheh, T. Sattler, R. Timofte, M. Pollefeys, and L. Van Gool. Night-to-day image translation for retrieval-based localization. *arXiv preprint arXiv:1809.09767*, 2018.
- [3] J.-R. Chang and Y.-S. Chen. Pyramid stereo matching network. In *Proceedings of the IEEE Conference on Computer Vision and Pattern Recognition*, pages 5410–5418, 2018.
- [4] I. Goodfellow, J. Pouget-Abadie, M. Mirza, B. Xu, D. Warde-Farley, S. Ozair, A. Courville, and Y. Bengio. Generative adversarial nets. In *Advances in neural information processing systems*, pages 2672–2680, 2014.

- [5] X. Guo, Y. Li, and H. Ling. Lime: Low-light image enhancement via illumination map estimation. *IEEE Transactions on Image Processing*, 26(2):982–993, 2017.
- [6] K. He, X. Zhang, S. Ren, and J. Sun. Spatial pyramid pooling in deep convolutional networks for visual recognition. In *European conference on computer vision*, pages 346–361. Springer, 2014.
- [7] K. He, X. Zhang, S. Ren, and J. Sun. Deep residual learning for image recognition. In *Proceedings of the IEEE conference on computer vision and pattern recognition*, pages 770–778, 2016.
- [8] Y. S. Heo, K. M. Lee, and S. U. Lee. Simultaneous depth reconstruction and restoration of noisy stereo images using non-local pixel distribution. In *Computer Vision and Pattern Recognition, 2007. CVPR’07. IEEE Conference on*, pages 1–8. IEEE, 2007.
- [9] H. Hirschmüller. Accurate and efficient stereo processing by semi-global matching and mutual information. In *Computer Vision and Pattern Recognition, 2005. CVPR 2005. IEEE Computer Society Conference on*, volume 2, pages 807–814. IEEE, 2005.
- [10] H. Hirschmüller and D. Scharstein. Evaluation of stereo matching costs on images with radiometric differences. *IEEE Transactions on Pattern Analysis & Machine Intelligence*, (9):1582–1599, 2008.
- [11] P. Isola, J.-Y. Zhu, T. Zhou, and A. A. Efros. Image-to-image translation with conditional adversarial networks. In *IEEE Conference on Computer Vision and Pattern Recognition*, 2017.
- [12] J. Jiao, Q. Yang, S. He, S. Gu, L. Zhang, and R. W. Lau. Joint image denoising and disparity estimation via stereo structure pca and noise-tolerant cost. *International Journal of Computer Vision*, 124(2):204–222, 2017.
- [13] J. Johnson, A. Alahi, and L. Fei-Fei. Perceptual losses for real-time style transfer and super-resolution. In *European Conference on Computer Vision*, pages 694–711. Springer, 2016.
- [14] A. Jolicœur-Martineau. The relativistic discriminator: a key element missing from standard gan. *arXiv preprint arXiv:1807.00734*, 2018.
- [15] A. Kendall, H. Martirosyan, S. Dasgupta, P. Henry, R. Kennedy, A. Bachrach, and A. Bry. End-to-end learning of geometry and context for deep stereo regression. *CoRR*, vol. abs/1703.04309, 2017.
- [16] D. Kinga and J. B. Adam. A method for stochastic optimization. In *International Conference on Learning Representations (ICLR)*, volume 5, 2015.
- [17] M.-Y. Liu, T. Breuel, and J. Kautz. Unsupervised image-to-image translation networks. In *Advances in Neural Information Processing Systems*, pages 700–708, 2017.
- [18] W. Maddern, G. Pascoe, C. Linegar, and P. Newman. 1 year, 1000 km: The oxford robotcar dataset. *The International Journal of Robotics Research*, 36(1):3–15, 2017.
- [19] X. Mao, Q. Li, H. Xie, R. Y. Lau, Z. Wang, and S. P. Smolley. Least squares generative adversarial networks. In *Computer Vision (ICCV), 2017 IEEE International Conference on*, pages 2813–2821. IEEE, 2017.
- [20] N. Mayer, E. Ilg, P. Häusser, P. Fischer, D. Cremers, A. Dosovitskiy, and T. Brox. A large dataset to train convolutional networks for disparity, optical flow, and scene flow estimation. In *IEEE International Conference on Computer Vision and Pattern Recognition (CVPR)*, 2016. arXiv:1512.02134.
- [21] M. Menze and A. Geiger. Object scene flow for autonomous vehicles. In *Proceedings of the IEEE Conference on Computer Vision and Pattern Recognition*, pages 3061–3070, 2015.
- [22] J. Pang, W. Sun, C. Yang, J. Ren, R. Xiao, J. Zeng, and L. Lin. Zoom and learn: Generalizing deep stereo matching to novel domains. In *The IEEE Conference on Computer Vision and Pattern Recognition (CVPR)*, June 2018.
- [23] G. Ros, L. Sellart, J. Materzynska, D. Vazquez, and A. M. Lopez. The synthia dataset: A large collection of synthetic images for semantic segmentation of urban scenes. In *The IEEE Conference on Computer Vision and Pattern Recognition (CVPR)*, June 2016.
- [24] D. Scharstein and R. Szeliski. A taxonomy and evaluation of dense two-frame stereo correspondence algorithms. *International journal of computer vision*, 47(1-3):7–42, 2002.
- [25] A. Sharma and L.-F. Cheong. Into the twilight zone: Depth estimation using joint structure-stereo optimization. In *Proceedings of the European Conference on Computer Vision (ECCV)*, pages 103–118, 2018.
- [26] A. Shrivastava, T. Pfister, O. Tuzel, J. Susskind, W. Wang, and R. Webb. Learning from simulated and unsupervised images through adversarial training. In *CVPR*, volume 2, page 5, 2017.
- [27] C. Zhang, Z. Li, Y. Cheng, R. Cai, H. Chao, and Y. Rui. Meshstereo: A global stereo model with mesh alignment regularization for view interpolation. In *Proceedings of the IEEE International Conference on Computer Vision*, pages 2057–2065, 2015.
- [28] H. Zhang, I. Goodfellow, D. Metaxas, and A. Odena. Self-attention generative adversarial networks. *arXiv preprint arXiv:1805.08318*, 2018.
- [29] J.-Y. Zhu, T. Park, P. Isola, and A. A. Efros. Unpaired image-to-image translation using cycle-consistent adversarial networks. In *Computer Vision (ICCV), 2017 IEEE International Conference on*, 2017.